Organic & Biomolecular Chemistry

PAPER

View Article Online
View Journal | View Issue

Cite this: *Org. Biomol. Chem.*, 2016, **14**, 1091

Diazaoxatriangulenium: synthesis of reactive derivatives and conjugation to bovine serum albumin†

Ilkay Bora, Sidsel A. Bogh, Martin Rosenberg, Marco Santella, Thomas Just Sørensen* and Bo W. Laursen*

Received 7th November 2015,
Accepted 26th November 2015

DOI: 10.1039/c5ob02293b

www.rsc.org/obc

The azaoxa-triangulenium dyes are characterised by emission in the red and a long fluorescence lifetime (up to 25 ns). These properties have been widely explored for the azadioxatrianguelnium (ADOTA) dye. Here, the syntheses of reactive maleimide and NHS-ester forms of the diazaoxatriangulenium (DAOTA) system are reported. The DAOTA fluorophore was conjugated to bovine serum albumin (BSA) and investigated in comparison to the corresponding ADOTA-BSA conjugate. It was found that the fluorescence of DAOTA experienced a significantly higher degree of solvent quenching if compared to ADOTA as non-conjugated dyes in aqueous solution, while the fluorescence quenching observed upon conjugation to BSA was significantly reduced for DAOTA when compared to ADOTA. The differences in observed quenching for the conjugates can be explained by the different electronic structures of the dyes, which renders DAOTA significantly less prone to reductive photoinduced electron transfer (PET) quenching from *e.g.* tryptophan. We conclude that DAOTA, with emission in the red and inherent resistance to PET quenching, is an ideal platform for the development of long fluorescence lifetime probes for time-resolved imaging and fluorescence polarisation assay.

Introduction

Fluorescence technology is prevalent in high-tech applications from diagnostics,[1,2] point-of-care devices,[3,4] and display technology to DNA sequencing,[5] drug-discovery,[6] and imaging.[7,8] Each application relies on dye development, be it bioengineered fluorescent proteins,[9] emissive nanoparticles,[10] inorganic luminophores,[11,12] or organic dyes.[13–16] Organic dye development is limited by fluorophore design, where many of the existing molecular frameworks have been known for more than a century.[17] Many dye systems have been synthesised using these well-known scaffolds,[18–21] and have been optimised to show significantly enhanced performance.[22–31] In particular, photostability, absorption cross-section, fluorescence quantum yield, and emission wavelength have been enhanced to the extent possible for the available fluorophores.

In the group of organic dyes, the triangulenium dyes are different.[32] In these molecules, a small absorption cross-section, and the resulting low fluorescence rate constant, does not infer low photostability and low quantum yield. While donor-substituted triangulenium dyes are bright emitters similar to rhodamine and fluorescein dyes,[33–36] the azaoxa-triangulenium dyes are highly photostable, highly emissive, long fluorescence lifetime dyes.[37–41] This group of triangulenium dyes includes azadioxatriangulenium (ADOTA) and diazaoxa-triangulenium (DAOTA) shown in Chart 1 (for details on the triangulenium nomenclature see ESI†). The aza-bridges are readily functionalised with groups compatible, with the reaction conditions used to form the aromatic core.

The triangulenium dyes are synthesised from common precursors using sequences of highly selective nucleophilic

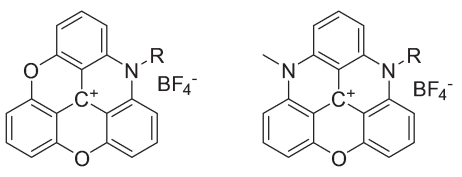

4.BF_4 **ADOTA** azadioxatriangulenium

5.BF_4 **DAOTA** diazaoxatriangulenium

Chart 1 The azaoxa-triangulenium dyes: ADOTA and DAOTA.

Nano-Science Center & Department of Chemistry, University of Copenhagen, Universitetsparken 5, 2100 København Ø, Denmark. E-mail: TJS@chem.ku.dk, bwl@nano.ku.dk

†Electronic supplementary information (ESI) available: Nomenclature of triangulenium ions, data for quantum yield determinations, labelling procedure, parameters describing the time-dependent photophysical properties, tryptophan quenching experiments, and NMR spectra. See DOI: 10.1039/c5ob02293b

aromatic substitution reactions (S_NAr).[33–35,38,42] For the azaoxatriangulenium dyes, each substitution step occurs in a cascade of two S_NAr-reactions forming a heteroatom bridge.[37,38] A similar approach has recently been used to form the aza-bridge in carbazoles.[43] Alternatively, ether-cleaving reaction conditions can be used to initiate an intramolecular S_NAr-reaction with the formation of an oxygen bridge.[44] Here, we elaborate on the synthesis of diazaoxatriangulenium (DAOTA) in an effort to make DAOTA derivatives, with reactive linkers for conjugation of the DAOTA fluorophore to biomolecules.

We chose to use bovine serum albumin (BSA) as a demonstrator for bioconjugation, although native BSA is not an ideal model system,[26,29,45] the results allow for a direct comparison between DAOTA and ADOTA BSA-conjugates.[46] We have previously investigated bioconjugates of ADOTA to BSA and IgG, and used both of the azaoxa-triangulenium dyes in bioimaging.[46–49] When conjugated to a biomolecule, the ADOTA fluorescence is significantly quenched. This has also been observed for other fluorophores and rationalised as photoinduced electron transfer (PET) quenching by tryptophan.[50–52] As DAOTA is less electron deficient than ADOTA,[38,53] it was expected that DAOTA would be much less prone to reductive PET quenching by tryptophan. This difference in PET activity between ADOTA and DAOTA was recently highlighted in a study of a DAOTA based DNA G-quadruplex fluorescence lifetime probe.[41] Here, we report a significant reduction in fluorescence quenching of DAOTA upon bio-conjugation, but also that the DAOTA dyes undergo significant solvent quenching, which leaves room for further improvements of this long fluorescent lifetime fluorophore. In particular, the solubility of DAOTA in water needs to be improved for several applications, in close analogy to what was achieved with the Alexa dyes®.[54–57]

Experimental

Materials and methods

Absorption spectroscopy was recorded with a double-beam spectrophotometer using the pure solvent as baseline. Steady state fluorescence spectra were recorded with a standard L-configuration fluorimeter equipped with single grating monochromators. All solvents used for spectroscopic experiments were of HPLC grade and used as received. Phosphate buffered saline (PBS) was prepared from slats according to common protocols. The pH value of the buffer was determined and subsequently adjusted to 7.4. Molar absorption coefficients were determined for each of the dyes using Lambert–Beers law by measuring the absorption spectrum of three stock solutions with different concentrations of the dye. Quantum yields were determined using the relative method,[58] using rhodamine 6G as standard (ϕ_{fl} = 0.95).[59] Details on the quantum yield measurements are given in the ESI.† Fluorescence lifetimes were measured using a FluoTime 300 (PicoQuant, Berlin, Germany) system. The emission signal was measured with a Hybrid-PMT detector with a spectral range of 220–650 nm. The dyes were excited at 510 nm using a solid-state laser excitation source. The instrument response function was recorded at the excitation wavelength using a dilute solution of Ludox®. The fluorescence decays were analyzed using the FluoFit software package. The decay data were all found to be monoexponential and was fitted by iterative reconvolution with a single exponential

$$I_f(t) = \alpha \exp(-t/\tau) \quad (1)$$

In eqn (1) α is the amplitude and τ is the fluorescence lifetime. All time-resolved emission decay profiles and fits are shown in the ESI.†

Synthetic procedures

Unless otherwise stated, all starting materials were obtained from commercial suppliers and used as received. Solvents were of HPLC grade for reactions and recrystallisations and technical grade for column chromatography and were used as received. ^{1}H NMR and ^{13}C NMR spectra were recorded on a 500 MHz or a 300 MHz instrument (500/300 MHz for ^{1}H NMR and 126 MHz for ^{13}C NMR). Proton chemical shifts are reported in ppm downfield from tetramethylsilane (TMS) and carbon chemical shifts in ppm downfield of TMS, using the resonance of the residual solvent peak as internal standard. High-resolution mass spectra (HRMS) were recorded with an ESP-MALDI-FT-ICR spectrometer equipped with a 7 T magnet (prior to experiments, the instrument was calibrated using NaTFA cluster ions) using dithranol as matrix. Column chromatographic purifications were performed on Kieselgel 60 (0.040–0.063 mm particle size). Dry column vacuum chromatography was performed on Kieselgel 60 (0.015–0.040 mm particle size). Thin layer chromatography was carried out using aluminum sheets pre-coated with silica gel 60F.

Synthesis of 2 and 4. Compound **1** was prepared according to the published procedure, see ref. 37. The compounds **2a–d** and **4a–d** were prepared as reported in ref. 47.

***N*-(3-Carboxypropyl)-*N*′-methyl-1,13-dimethoxy-quin[2,3,4-*kl*]-acridinium tetrafluoroborate 3a.** 1,8-Dimethoxy-10-(2,6-dimethoxyphenyl)-9-(3-carboxypropyl)-acridinium methyl ester tetrafluoroborate **2a** (0.5 g, 0.9 mmol) was placed in a sealable tube and dissolved in acetonitrile (5 mL) and excess methylamine (15 mL, 33 wt% in ethanol) was added. The solution was stirred at 60 °C for five days. After it had cooled to ambient temperature it was poured into diethyl ether (500 mL) to precipitate the product. The crude material was dissolved in potassium hydroxide solution (1 M, 0.1 L) and stirred at refluxing conditions for 5 h. After cooling aqueous tetrafluoroboric acid (50 wt% in water) was used to acidify the solution when a dark precipitate formed, which was filtered off. The crude compound was dissolved in warm acetonitrile, filtered through a paper filter, and precipitated twice from a solution of acetonitrile with diethyl ether. Recrystallisation from *i*-propanol/acetonitrile and yielded dark green crystals, which are washed with dichloromethane and dried in vacuum (0.315 g, 69%). **^{1}H NMR** (500 MHz, Acetonitrile-d_3) δ 8.10 (t, J = 8.4 Hz, 1H), 7.91 (t, J = 8.5 Hz, 1H), 7.86 (t, J = 8.4 Hz, 1H), 7.72 (d, J = 8.6 Hz,

1H), 7.67 (d, J = 8.9 Hz, 1H), 7.43–7.34 (m, 2H), 6.93–6.84 (m, 2H), 4.78–4.68 (m, 1H), 4.53–4.43 (m, 1H), 4.02 (s, 3H), 3.72 (s, 3H), 3.71 (s, 3H), 2.68 (t, J = 6.3 Hz, 2H), 2.34–2.19 (m, 2H). **^{13}C NMR** (126 MHz, Acetonitrile-d_3) δ 175.2, 160.5, 160.2, 143.7, 143.3, 143.1, 140.6, 139.7, 138.1, 137.8, 137.3, 120.1, 113.9, 113.9, 108.6, 108.5, 106.0, 105.8, 104.1, 104.0, 56.5, 38.2, 31.2, 21.9. **HRMS (MALDI-TOF):** m/z calcd for $C_{26}H_{25}N_2O_4^+$, 429.1809; found, 429.1811.

***N*-[2-(4-Carboxyphen)ethyl]-*N*′-methyl-1,13-dimethoxy-quin-[2,3,4-*kl*]acridinium tetrafluoroborate 3b.** 1,8-Dimethoxy-10-(2,6-dimethoxyphenyl)-9-(2-(4-carboxyphenyl)-ethyl)-acridinium tetrafluoroborate **2b** (0.35 g, 0.60 mmol) was placed in a sealable tube and dissolved in acetonitrile (10 mL) and methylamine (12 mL, 33 wt% in ethanol) was added. The tube was sealed and the mixture was stirred at 65 °C for three days. After cooling to ambient temperature the solution was poured into diethyl ether to precipitate the compound. It was then dissolved in sodium hydroxide solution (1 M, 50 mL) and extracted three times with dichloromethane. Then the pH value was adjusted to ~3 with tetrafluoroboric acid (50 wt% in water) to precipitate the product. The material was dissolved in dichloromethane and filtered. The solvent was removed in vacuum. The material was subsequently precipitated twice from a solution of acetonitrile with diethyl ether to give the compound as blue powder which was washed with dichloromethane, and dried in vacuum (0.271 g, 78%). **^{1}H NMR** (300 MHz, Methanol-d_4) δ 8.22 (t, J = 8.5 Hz, 1H), 7.98–7.86 (m, 2H), 7.80–7.67 (m, 3H), 7.60 (d, J = 8.5 Hz, 1H), 7.57 (d, J = 4.0 Hz, 1H), 7.54 (d, J = 4.0 Hz, 1H), 7.23 (s, 2H), 7.00 (d, J = 8.1 Hz, 1H), 6.96 (d, J = 8.0 Hz, 1H), 5.20–4.99 (m, 2H), 4.18 (s, 3H), 3.78 (s, 3H), 3.76 (s, 3H), 3.42–3.34 (m, 2H). **^{13}C NMR** (126 MHz, Methanol-d_4) δ 169.4, 161.0, 160.7, 144.2, 143.8, 143.8, 143.5, 140.9, 139.8, 138.4, 138.2, 137.6, 131.0, 130.5, 130.1, 120.4, 114.7, 114.6, 108.8, 108.7, 106.6, 106.4, 104.3, 104.1, 56.3, 56.2, 37.9, 33.6. **HRMS (MALDI-TOF):** m/z calcd for $C_{31}H_{27}N_2O_4^+$, 491.1965; found, 491.1942.

1,13-Dimethoxy-*N*-(4-(methylcarbamoyl)phenyl)-*N*′-methyl-quin[2,3,4-*kl*]acridinium tetrafluoroborate 3c′. 1,8-Dimethoxy-10-(2,6-dimethoxyphenyl)-9-(4-carboxyphenyl)-acridinium methyl ester tetrafluoroborate **2c** (0.69 g, 1.16 mmol) was placed in a round bottom flask (100 mL) and dissolved in methylamine (50 mL, 33 wt% ethanol). The flask was equipped with a reflux condenser fitted with a balloon to trap the evaporating gas. The solution was stirred at 70 °C for three days. After cooling the mixture was poured into diethyl ether to precipitate the crude product. Column chromatography over silica (dichloromethane/methanol 10/1) yielded the product as green powder, which was washed with diethyl ether and dried in vacuum (0.31 g, 48%). ^{1}H NMR (500 MHz, Methanol-d_4) δ 8.27 (d, J = 8.6 Hz, 2H), 8.05–7.96 (m, 2H), 7.72 (t, J = 8.4 Hz, 2H), 7.70–7.65 (m, 1H), 7.62 (t, J = 8.5 Hz, 3H), 7.05 (d, J = 8.1 Hz, 1H), 6.99 (d, J = 8.0 Hz, 1H), 6.70 (d, J = 8.5 Hz, 1H), 6.57 (d, J = 8.7 Hz, 1H), 4.23 (s, 3H), 3.82 (s, 6H), 3.02 (s, 3H). ^{13}C NMR (126 MHz, Methanol-d_4) δ 169.1, 161.1, 161.1, 153.8, 145.1, 144.8, 144.6, 142.0, 141.2, 141.0, 138.8, 138.0, 138.0, 137.4, 120.0, 115.0, 113.98, 109.7, 108.9, 107.3, 106.7, 104.5, 104.5, 101.6, 56.4, 56.3, 38.0, 27.1. HRMS (MALDI-TOF): m/z calcd for $C_{30}H_{26}N_3O_3^+$: 476.1969; found, 476.1972.

***N*-(4-Aminophenyl)-*N*′-methyl-1,13-dimethoxy-quin[2,3,4-*kl*]-acridinium tetrafluoroborate 3d.** 1,8-Dimethoxy-10-(2,6-dimethoxyphenyl)-9-(4-aminophenyl)-acridinium tetrafluoroborate **2d** (0.55 g, 1.00 mmol) was placed in a sealed round bottom flask and was dissolved in acetonitrile (10 mL) and methylamine (14 mL, 33% in EtOH) equipped with a reflux condenser fitted with a balloon to trap evaporating gas. The mixture was stirred under refluxing conditions. Over two days the solution turned dark green and additional methylamine (15 mL) was added. After a total of three days at refluxing conditions the solution was cooled to ambient temperature and poured into diethyl ether (500 mL) to precipitate the product. Precipitation was repeated from a solution of acetonitrile with diethyl ether to give the crude green product. The material was first recrystallized from *i*-propanol/acetonitrile and further purified by dry column chromatography (silica; heptane → CH_2Cl_2 → CH_3CN → *i*-propanol) to give the dark green product (0.387 g, 74%). **^{1}H NMR** (500 MHz, Acetonitrile-d_3) δ 7.98 (t, J = 8.5 Hz, 1H), 7.94–7.90 (m, 1H), 7.72–7.68 (m, 1H), 7.51–7.43 (m, 2H), 7.22 (dd, J = 8.4, 2.6 Hz, 1H), 7.07 (dd, J = 8.5, 2.6 Hz, 1H), 7.01 (dd, J = 8.5, 2.6 Hz, 1H), 6.98–6.94 (m, 2H), 6.90 (d, J = 8.0 Hz, 1H), 6.83 (d, J = 8.5 Hz, 1H), 6.74 (d, J = 8.8 Hz, 1H), 4.71 (s, 2H), 4.11 (s, 3H), 3.78 (s, 3H), 3.77 (s, 3H). **^{13}C NMR** (126 MHz, Acetonitrile-d_3) δ 160.5, 160.4, 150.9, 145.3, 144.4, 144.3, 142.0, 140.6, 138.0, 137.5, 136.9, 130.9, 129.3, 127.9, 120.0, 117.3, 116.7, 114.2, 113.6, 110.2, 108.7, 107.5, 106.0, 104.2, 104.0, 56.6, 56.6, 38.2. **HRMS (MALDI-TOF):** m/z calcd for $C_{28}H_{24}N_3O_2^+$, 434.1863; found, 434.1849.

***N*-(3-Carboxypropyl)-*N*′-methyl-diazaoxatriangulenium tetrafluoroborate 5a.** *N*-(3-Carboxypropyl)-*N*′-methyl-1,13-dimethoxy-quin[2,3,4-*kl*]acridinium tetrafluoroborate **3a** (3.0 g, 5.8 mmol) dissolved in pyridine (4 mL) was added to molten pyridinium chloride (20 g) at 170 °C and stirred for 135 min. The product was precipitated by addition of sodium tetrafluoroborate solution (0.2 M, 0.5 L) and filtered off. The crude compound was dissolved in hot acetonitrile and filtered through a paper filter. Twofold precipitation of the product from a solution of acetonitrile with diethyl ether and recrystallisation from acetonitrile gave the compound as red solid (2.26 g, 83%). **^{1}H NMR** (500 MHz, Acetonitrile-d_3) δ 8.22 (t, J = 8.6 Hz, 1H), 8.08–8.04 (m, 1H), 8.04–8.01 (m, 1H), 7.64 (d, J = 8.8 Hz, 1H), 7.56 (d, J = 8.6 Hz, 1H), 7.49 (d, J = 8.8 Hz, 1H), 7.40 (d, J = 8.6 Hz, 1H), 7.28–7.19 (m, 2H), 4.48–4.42 (m, 2H), 3.89 (s, 3H), 2.65 (t, J = 6.6 Hz, 2H), 2.11–2.09 (m, 2H, overlap with residual water in CD_3CN). **^{13}C NMR** (126 MHz, Acetonitrile-d_3) δ 173.4, 152.1, 141.2, 140.4, 140.0, 139.3, 139.3, 138.2, 138.1, 117.0, 109.0, 108.8, 108.1, 108.0, 107.0, 105.7, 105.4, 46.9, 35.1, 29.1, 19.8. **HRMS (MALDI-TOF):** m/z calcd for $C_{24}H_{19}N_2O_3^+$, 383.1390; found, 383.1394.

***N*-[2-(4-Carboxyphen)ethyl]-*N*′-methyl-diazaoxatriangulenium tetrafluoroborate 5b.** *N*-(2-(4-Carboxyphenyl)-ethyl)-azadioxatriangulenium tetrafluoroborate **4b** (0.09 g, 0.17 mmol) was placed in a sealable tube and dissolved in *N*-methyl-2-pyrrolidone

(4 mL) and methylamine (1 mL, 8.7 mmol, 33 wt% in ethanol). The solution was stirred at 85 °C overnight. After 15 h the solution was colored red and a precipitate formed, which was filtered off. The solution was poured into sodium tetrafluoroborate solution (0.2 M, 0.1 L) and the pH was adjusted to ~3 with tetrafluoroboric acid (50 wt% in water) to precipitate the remaining product. The crude product was washed with water, dissolved in hot acetonitrile and filtered through a paper filter. After cooling the material was precipitated with diethyl ether. Repeated precipitation from a solution of acetonitrile with diethyl ether yielded the pure compound as a fine red powder, which was dried under vacuum (0.04 g, 43%). **^{1}H NMR** (500 MHz, DMSO-d_6) δ 8.25 (t, J = 8.4 Hz, 1H), 8.08 (m, 2H), 7.87 (d, J = 8.0 Hz, 2H), 7.70–7.65 (m, 2H), 7.60–7.53 (m, 4H), 7.34–7.29 (m, 2H), 4.81–4.74 (m, 2H), 3.95 (s, 3H), 3.22–3.16 (m, 2H). **^{13}C NMR** (126 MHz, DMSO-d_6) δ 167.2, 151.8, 151.7, 142.1, 141.0, 139.9, 139.8, 139.6, 139.0, 139.0, 138.5, 138.4, 129.8, 129.5, 118.1, 110.8, 109.6, 109.5, 108.3, 108.1, 107.0, 106.3, 106.0, 47.6, 35.6, 31.1. **HRMS (MALDI-TOF):** m/z calcd for $C_{29}H_{21}N_2O_3^+$, 445.1547; found, 445.1549.

***N*-(4-Carboxyphenyl)-*N*′-methyl-diazaoxatriangulenium tetrafluoroborate 5c.** *N*-(4-Carboxyphenyl)-azadioxatriangulenium tetrafluoroborate **4c** (0.11 g, 0.23 mmol) and benzoic acid (0.6 g, 4.9 mmol) were placed in a round bottom flask and dissolved in ethanol (5 mL) and methylamine (0.57 mL, 4.6 mmol, 33 wt% in ethanol). The mixture was heated to reflux overnight. After 18 h additional methylamine (0.5 mL) was added and reflux of the mixture was continued for another day. Sodium tetrafluoroborate solution (0.2 M, 0.1 L) was added to precipitate the product. The red material was dissolved in dichloromethane, dried over sodium sulfate, and filtered. Repeated precipitation from a solution of acetonitrile with diethyl ether and drying in vacuum gave the pure product as a dark red powder (0.1 g, 86%). **^{1}H NMR** (500 MHz, DMSO-d_6) δ 8.41 (d, J = 8.1 Hz, 2H), 8.20 (t, J = 8.5 Hz, 1H), 8.12 (t, J = 8.5 Hz, 1H), 7.95 (t, J = 8.4 Hz, 1H), 7.85 (d, J = 8.8 Hz, 1H), 7.74 (d, J = 8.1 Hz, 2H), 7.68 (d, J = 8.7 Hz, 1H), 7.49 (d, J = 8.1 Hz, 1H), 7.45 (d, J = 8.2 Hz, 1H), 6.60 (d, J = 8.6 Hz, 1H), 6.53 (d, J = 8.4 Hz, 1H), 4.09 (s, 3H). **^{13}C NMR** (126 MHz, DMSO-d_6) δ 166.5, 152.1, 151.9, 144.7, 141.7, 141.0, 140.5, 140.5, 140.3, 140.1, 139.4, 138.9, 138.4, 133.04, 128.9, 110.8, 110.1, 108.6, 108.5, 107.5, 107.1, 106.7, 106.7, 35.7. **HRMS (MALDI-TOF):** m/z calcd for $C_{27}H_{17}N_2O_3^+$, 417.1234; found, 417.1236.

***N*-(4-Aminophenyl)-*N*′-methyl-diazaoxatriangulenium tetrafluoroborate 5d.** Pyridinium chloride (36 g) was heated to 185 °C and *N*-(4-aminophenyl)-*N*′-methyl-1,13-dimethoxy-quin[2,3,4-*kl*]acridinium tetrafluoroborate **3d** (0.94 g, 1.84 mmol) was added and stirred for 45 minutes. After completion of the reaction sodium tetrafluoroborate solution (0.2 M, 0.4 L) was added (pH adjusted to 9 with sodium hydroxide solution) to precipitate the product. After cooling to ambient temperature the material was filtered off and washed with additional sodium tetrafluoroborate solution and water. Precipitation of the compound from a solution of acetonitrile with diethyl ether gave a fine powder which was recrystallized from *i*-propanol/methanol to yield the pure compound as dark crystals which are washed with cold acetonitrile and methanol (0.15 g, 17.5%). **^{1}H NMR** (500 MHz, DMSO-d_6) δ 8.17–8.09 (m, 2H), 7.96 (t, J = 8.4 Hz, 1H), 7.77 (d, J = 8.9 Hz, 1H), 7.59 (d, J = 8.6 Hz, 1H), 7.44–7.37 (m, 2H), 7.15 (d, J = 8.6 Hz, 2H), 6.93 (d, J = 8.6 Hz, 2H), 6.73 (d, J = 8.7 Hz, 1H), 6.67 (d, J = 8.5 Hz, 1H), 5.78 (s, 2H), 4.03 (s, 3H). **^{13}C NMR** (126 MHz, DMSO-d_6) δ 152.1, 151.8, 150.6, 142.8, 141.6, 140.9, 140.3, 139.7, 139.2, 138.6, 138.1, 128.5, 124.5, 115.8, 111.0, 110.5, 109.9, 108.3, 108.2, 107.3, 107.1, 107.0, 106.1, 35.6. **Anal. Calcd** for $C_{26}H_{18}BF_4N_3O$: C, 65.71; H, 3.82; N, 8.84; Found: C, 65.94; H, 3.54; N, 9.10. **HRMS (MALDI-TOF):** m/z calcd for $C_{26}H_{18}N_3O^+$, 388.1444; found, 388.1455.

***N*-(3-Carboxypropyl)-*N*′-methyl-diazaoxatriangulenium NHS ester tetrafluoroborate 6a.** *N*-(3-Carboxypropyl)-*N*′-methyl-diazaoxatriangulenium tetrafluoroborate **5a** (0.20 g, 0.42 mmol), *N*,*N*,*N*′,*N*′-tetramethyl-*O*-(*N*-succinimidyl)uronium tetrafluoroborate (0.17 g, 0.55 mmol) and diisopropylethylamine (0.12 mL, 0.68 mmol) were dissolved in DMSO (20 mL) and stirred at ambient temperature overnight. The product was precipitated by addition of sodium tetrafluoroborate solution (0.2 M, 0.25 L) and filtered off. Then the crude material was redissolved in dichloromethane and a minor volume acetonitrile and dried over sodium sulfate, filtered, and the solvent was removed in vacuum. Precipitation from a solution of acetonitrile with diethyl ether gave a fine powder, which was purified by column chromatography (dichloromethane/methanol 19 : 1) to yield the compound as a red powder, which is washed with dichloromethane and dried in vacuum (0.11 g, 45%). **^{1}H NMR** (500 MHz, Acetonitrile-d_3) δ 8.20 (t, J = 8.6 Hz, 1H), 8.04–8.01 (m, 1H), 8.01–7.97 (m, 1H), 7.57 (d, J = 8.7 Hz, 1H), 7.50 (d, J = 8.6 Hz, 1H), 7.44 (d, J = 8.8 Hz, 1H), 7.36 (d, J = 8.6 Hz, 1H), 7.19 (d, J = 7.7 Hz, 1H), 7.15 (d, J = 7.8 Hz, 1H), 4.43–4.35 (m, 2H), 3.84 (s, 4H), 3.73 (s, 3H), 2.66 (t, J = 6.6 Hz, 2H), 2.12–2.09 (m, 2H). **^{13}C NMR** (126 MHz, Acetonitrile-d_3) δ 174.4, 153.3, 153.2, 142.4, 141.6, 141.2, 140.7, 140.6, 140.3, 139.6, 139.5, 118.0, 112.1, 110.3, 110.1, 109.5, 109.4, 108.3, 108.1, 107.0, 106.8, 52.5, 48.1, 36.4, 30.8, 21.2. **HRMS (MALDI-TOF):** m/z calcd for $C_{28}H_{22}N_3O_5^+$, 480.1554; found, 480.1550.

***N*-[2-(4-Carboxyphen)ethyl]-*N*′-methyl-diazaoxatriangulenium NHS ester tetrafluoroborate 6b.** *N*-[2-(4-Carboxyphen)ethyl]-*N*′-methyl-diazaoxatriangulenium tetrafluoroborate **5b** (0.10 g, 0.19 mmol) and *N*,*N*,*N*′,*N*′-tetramethyl-*O*-(*N*-succinimidyl)-uronium tetrafluoroborate (0.085 g, 0.28 mmol) were dissolved in acetonitrile (8 mL) and triethylamine (0.06 mL, 0.34 mmol). The solution was stirred at ambient temperature for 90 min. Then the product was precipitated with diethyl ether and filtered off. Washing with water (10 mL) and threefold precipitation from a solution of acetonitrile with diethyl ether gave the pure product as red powder (0.108 g, 91%). **^{1}H NMR** (500 MHz, Acetonitrile-d_3) δ 8.17 (t, J = 8.6 Hz, 1H), 8.05–8.00 (m, 2H), 7.97 (t, J = 8.5 Hz, 1H), 7.53 (d, J = 8.2 Hz, 2H), 7.48 (d, J = 8.8 Hz, 1H), 7.42 (d, J = 8.8 Hz, 1H), 7.38 (dd, J = 8.6, 5.9 Hz, 2H), 7.21 (d, J = 3.7 Hz, 1H), 7.19 (d, J = 3.8 Hz, 1H),

4.66 (t, J = 7.8 Hz, 2H), 3.88 (s, 3H), 3.29 (t, J = 7.7 Hz, 2H), 2.85 (s, 4H). **^{13}C NMR** (126 MHz, Acetonitrile-d_3) δ 171.2, 153.4, 153.3, 146.2, 142.5, 141.4, 141.2, 140.6, 140.4, 139.6, 139.5, 124.7, 112.1, 110.3, 110.2, 109.6, 109.4, 108.3, 107.2, 106.9, 48.8, 36.5, 32.4, 26.5. **HRMS (MALDI-TOF):** m/z calcd for $C_{33}H_{24}N_3O_5^+$, 542.1710; found, 542.1709.

***N*-(4-Carboxyphenyl)-*N*′-methyl-diazaoxatriangulenium NHS ester tetrafluoroborate 6c.** *N*-(4-Carboxyphenyl)-*N*′-methyl-diazaoxatriangulenium tetrafluoroborate 5c (0.04 g, 0.08 mmol) was placed in a flask and dissolved in DMSO (10 mL) and diisopropylethylamine (0.05 mL, 0.32 mmol). *N*,*N*,*N*′,*N*′-Tetramethyl-*O*-(*N*-succinimidyl)uronium tetrafluoroborate (0.05 g, 0.16 mmol) was added and the solution was stirred at ambient temperature overnight. After confirmation of product formation by MALDI-TOF analysis the material was precipitated by addition of sodium tetrafluoroborate solution (0.2 M, 0.1 L) and filtered off. The crude red material was dissolved in dichloromethane, dried over magnesium sulfate, filtered, and the solvent was evaporated in vacuum. Then the material was precipitated from a solution of acetonitrile with diethyl ether and dried in vacuum to give a red powder (0.016 g, 34%). ^{1}H NMR (500 MHz, Acetonitrile-d_3) δ 8.17 (t, J = 8.9 Hz, 1H), 8.06–8.00 (m, 3H), 7.97 (t, J = 8.5 Hz, 1H), 7.53 (d, J = 8.2 Hz, 2H), 7.48 (d, J = 8.8 Hz, 1H), 7.42 (d, J = 8.8 Hz, 1H), 7.40–7.35 (m, 2H), 7.21 (d, J = 3.7 Hz, 1H), 7.19 (d, J = 3.8 Hz, 1H), 4.66 (t, J = 7.8 Hz, 2H), 3.88 (s, 3H), 3.29 (t, J = 7.7 Hz, 2H), 2.85 (s, 4H).^{13}C NMR (126 MHz, Acetonitrile-d_3) δ 140.2, 139.8, 139.2, 135.0, 130.9, 111.1, 110.6, 109.8, 109.6, 107.9, 107.5, 36.5, 26.4. HRMS (MALDI-TOF): m/z calcd for $C_{31}H_{20}N_3O_5^+$, 514.1397; found, 514.1399.

***N*-(4-Malimidophenyl)-*N*′-methyl-diazaoxatriangulenium tetrafluoroborate 7.** *N*-(4-Aminophenyl)-*N*′-methyl-diazaoxatriangulenium tetrafluoroborate **5d** (0.1 g, 0.2 mmol) was placed in a round bottom flask and dissolved in acetonitrile (25 mL) and 2,6-lutidine (0.2 mL). After the compound dissolved completely maleic anhydride (0.1 g, 1 mmol) was added and the solution was refluxed for 4 h until all starting material was converted to the acid. The solvent was removed by evaporation and the acid was dissolved in acetic anhydride (8 mL) and stirred at 100 °C. After 30 min the reaction was completed and the solution was cooled to ambient temperature. The crude product was precipitated by addition of sodium tetrafluoroborate solution (0.2 M, 0.3 L). After filtration the material was dissolved in warm acetonitrile, filtered and precipitated with diethyl ether twice to yield the product as a fine red powder (0.08 g, 66%). **^{1}H NMR** (500 MHz, DMSO-d_6) δ 8.24–8.20 (m, 1H), 8.20–8.15 (m, 1H), 8.01 (t, J = 8.4 Hz, 1H), 7.92–7.88 (m, 2H), 7.88–7.86 (m, 1H), 7.78 (d, J = 8.9 Hz, 2H), 7.70 (d, J = 8.7 Hz, 1H), 7.52 (d, J = 8.2 Hz, 1H), 7.48 (d, J = 8.2 Hz, 1H), 7.32 (s, 2H), 6.60 (d, J = 8.7 Hz, 1H), 6.53 (d, J = 8.4 Hz, 1H), 4.11 (s, 3H). **^{13}C NMR** (126 MHz, DMSO-d_6) δ 169.7, 152.1, 151.9, 142.0, 141.0, 140.8, 140.4, 140.1, 135.9, 135.0, 133.6, 129.7, 129.7, 129.7, 129.2, 129.2, 110.8, 110.1, 108.5, 108.5, 107.6, 107.1, 106.7, 106.7, 106.6, 35.7. **HRMS (MALDI-TOF):** m/z calcd for $C_{30}H_{18}N_3O_3^+$; 468.1343; found, 468.1359.

Labelling procedure. Labelling of bovine serum albumin (BSA) was achieved either by activating the free carboxylic acid substituted dyes with *O*-(*N*-succinimidyl)-*N*,*N*,*N*′,*N*′-tetramethyluronium tetrafluoroborate (TSTU) in the presence of diisopropylethylamine (DIPEA), resulting in *in situ* formation of the *N*-hydroxysuccinimide (NHS) ester, which was subsequently reacted with BSA. Alternatively, NHS esters of the dyes were used directly. The BSA conjugates were subsequently purified by dialysis. Consult ref. 46 for the full labelling protocols and procedures. Despite the tendency of BSA to bind small molecules electrostatically, we did not observe unbound dye in the optical experiments.

Results and discussion

Synthesis

The synthesis of azaoxa-triangulenium dyes was developed in our lab,[37,38] based on the work of Martin and Smith,[44] who first synthesised the trioxatriangulenium (TOTA) system. In our early work, azadioxa-, diazaoxa-, and triaza-triangulenium (ADOTA, DAOTA, and TATA) was reported.[37,38] Lacour and co-workers have later expanded the series of triangulenium salts to also include derivatives with a single sulfur bridge.[60] The incorporation of more than one sulfur atom in the triangulenium core seems not to be possible due to the distortion enforced by the significantly different C–S bond length as compared to C–N and C–O bonds.[61] The azaoxa-triangulenium dyes are all made from a common precursor; tris(2,6-dimethoxyphenyl)-carbenium tetrafluoroborate (**1**) which, can be reacted stepwise with primary amines to form between one and three aza-bridges. **1** or each intermediate may be reacted under ether cleaving conditions at elevated temperatures to form the fully ring closed triangulenium core with one, two, or three oxa-bridges. The oxa-bridges are themselves reactive towards primary amines. However, this substitution reaction is slow compared to attack on the methoxy groups of the open precursors, but it is still highly selective.[38]

Post-functionalisation of the substituents on the aza-bridges have previously been reported,[62,63] and we have synthesised and explored reactive derivatives of ADOTA for bioconjugation.[46,48,49]

The syntheses of ADOTA with reactive NHS esters and maleimide groups (Scheme 1) are straightforward, and proceed by a S_NAr reaction between **1** and a suitable amino acid or diamine. The primary amine attack one of the methoxy substituted carbon atoms in **1** followed by elimination of methanol upon formation of a transient intermediate set up for an intramolecular S_NAr reaction, eliminating methanol and forming an aza-bridge. The product is an *N*-substituted tetramethoxy-acridinium salt (**2**). Reacting **2** in molten pyridinium chloride yields the fully ring closed azadioxa-triangulenium (**4**, ADOTA).[37,38] Alternatively, a second aza-bridge can be introduced by reacting **2** with a second primary amine forming a [4]helicenium ion. The product is an *N*,*N*′-substituted 1,13-dimethoxyquinacridinium (DMQA) salt (**3**, for details on this nomenclature see

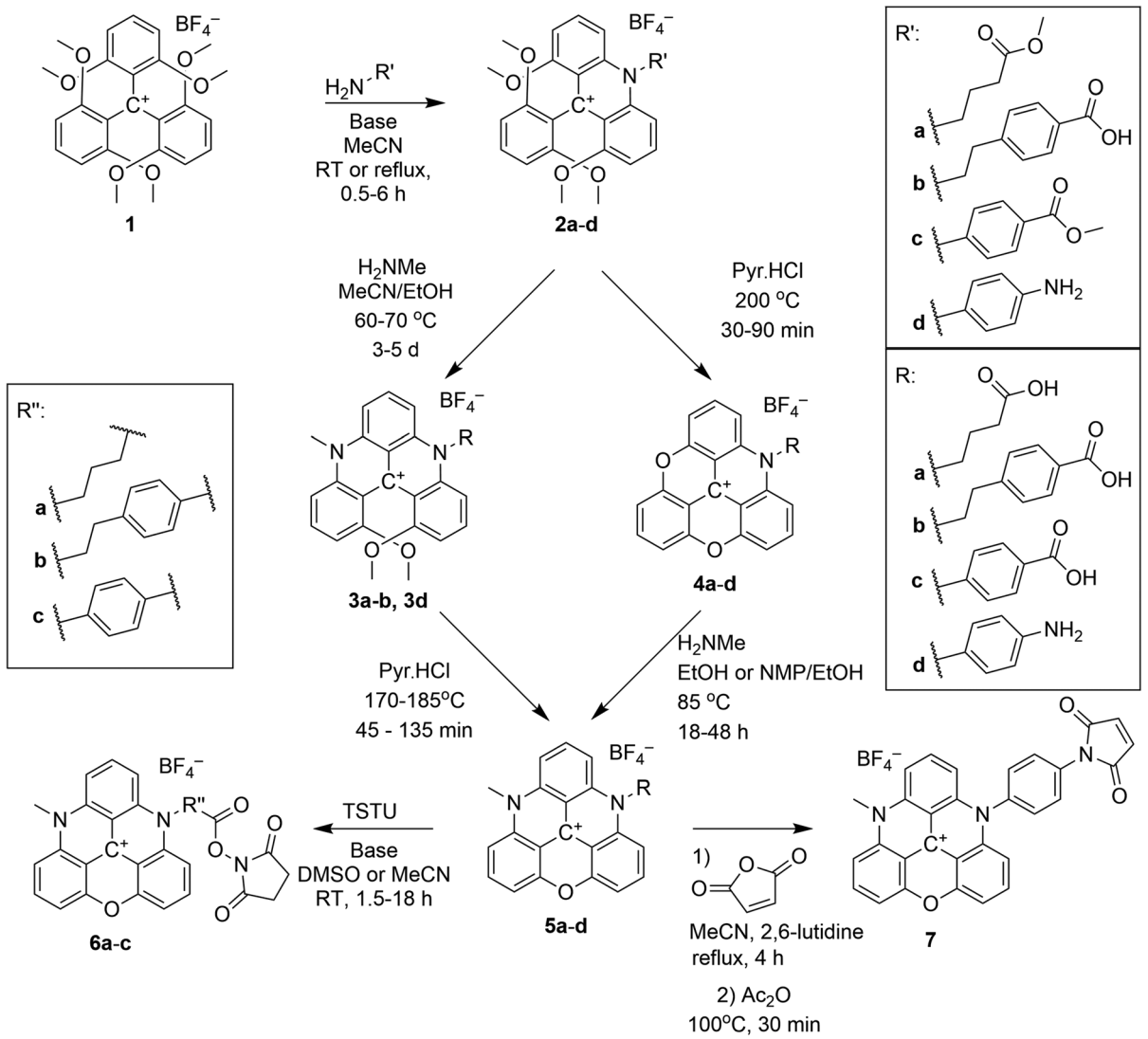

Scheme 1 Synthetic route to DAOTA compounds: **5a–d**, **6a–c**, and **7**.

ESI†), which in molten pyridinium chloride yields the fully ring closed diazaoxa-triangulenium core (**5**, DAOTA).

The steps to ADOTA-derivatives suitable for bioconjugation as active esters and maleimides follow the direct path from **1** over **2** to **4**.[47] Similarly, the 3-carboxypropyl derivative of DAOTA (**2a**) could be synthesised by introducing first one (**2a**), and then a second aza-bridge to give the DMQA derivative (**3c**). Subsequent reaction of the DMQA compounds in molten pyridinium chloride followed by basic hydrolysis of the intermediate amide yielded the desired *N*-(3-carboxypropyl)-*N*′-methyl-DAOTA tetrafluoroborate (**5a**, Scheme 1) as a red powder in a good yield.[49] The synthesis of the 4-aminophenyl DAOTA derivative (**5d**) was also performed *via* the route through the DMQA derivative (**3d**, Scheme 1). This yielded **3d** in a high yield, while the ring closure reaction for conversion of **3d** into **5d** yielded **5d** in a low yield. In attempts to prepare the 2-(4-carboxyphenyl)-ethyl and 4-carboxyphenyl DAOTA derivatives (**5b** and **5c**, respectively) *via* the same synthetic route as described for **5a** and **5d**, we found that this was associated with difficulties. The compound **3b** was isolated in a high yield. However, the following ring-closure reaction in molten pyridinium chloride yielded the desired product (**5b**) in combination with impurities, which were inseparable from **5b**. Similarly, the DMQA derivative **3c** could not be prepared as the basic hydrolysis of the intermediate amide derivative (**3c**′, Scheme 2) was not successful.

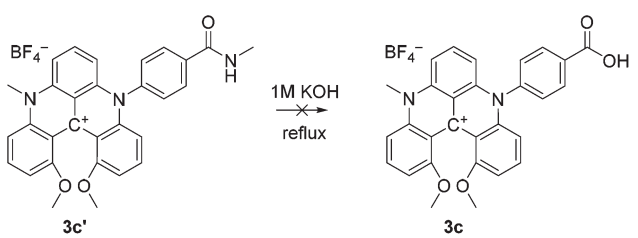

Scheme 2 Hydrolysis of DMQA amide **3c**′.

Thus, **5b** and **5c** were synthesised *via* an alternative route, which to our knowledge has only been reported for the *N*,*N*′-dipropyl-DAOTA salt by Laursen and Krebs.[38] The compounds **5b** and **5c** were obtained in good yields *via* reaction of the ADOTA derivatives (**4b** and **4c**) with methylamine in acetonitrile/ethanol or NMP/ethanol mixtures. The acid derivatives **5a–c** were reacted with *N*,*N*,*N*′,*N*′-Tetramethyl-*O*-(*N*-succinimidyl)uronium tetrafluoroborate (TSTU) in acetonitrile or DMSO solution to form the reactive NHS esters (**6a–c**) in good yields. The NHS ester functional group is used to conjugate fluorescent dyes to biomacromolecules *via* coupling to a primary amine residue of the biomacromolecule.[64]

Compound **5d** was reacted with maleic acid anhydride to form the corresponding maleimide **7** in a two-step/one pot reaction (Scheme 1).[47] The maleimide group is used to selectively label thiol groups in biomolecules.[64]

Optical spectroscopy

In the following *N*-(4-carboxyphenyl)-*N*′-methyl-DAOTA tetrafluoroborate **5c** is used to demonstrate the spectroscopic properties of the reactive DAOTA derivatives. The properties of **5c** are compared to those of the corresponding *N*-(4-carboxyphenyl)-ADOTA tetrafluoroborate **4c**.[46,47] The spectra displayed in Fig. 1 show that DAOTA (**5c**) has more desirable absorption and emission properties. These are in the red region of spectrum, which is better for measurements on biological systems as compared to ADOTA (**4c**).[49,53,65] Table 1 summarises the photophysical properties of **4c** and **5c** in acetonitrile, dimethyl sulfoxide (DMSO), and phosphate buffered saline at pH = 7.4 (PBS). The differences between **4c** and **5c** in organic solvents are closely related to the oscillator strengths of the lowest energy transition of the two parent chromophores. The higher molar absorption coefficient at the lowest energy transition of DAOTA as compared that of ADOTA (ε = 16 000 *vs.* 10 000 M^{-1} cm^{-1} in acetonitrile solution),[65] results in a shorter fluorescence lifetime (τ_{fl} = 19 *vs.* 21 ns in MeCN).[65,66] In PBS solution, DAOTA **5c** exhibits a significant change in fluorescence lifetime (τ_{fl}) and fluorescence quantum yield (ϕ_{fl}), where both are reduced; ϕ_{fl} from 55% to 35% and τ_{fl} from 19 ns to 14 ns. We have found that chloride is not a specific quencher of DAOTA, and suggest that the observed 30% reduction in ϕ_{fl} must be due to unspecific solvent quenching, likely due to the high hydrophobicity of the DAOTA core of **5c**. ADOTA **4c** is less hydrophobic and does not show more than 18% reduction in ϕ_{fl} in PBS solution as compared to the organic solvents.

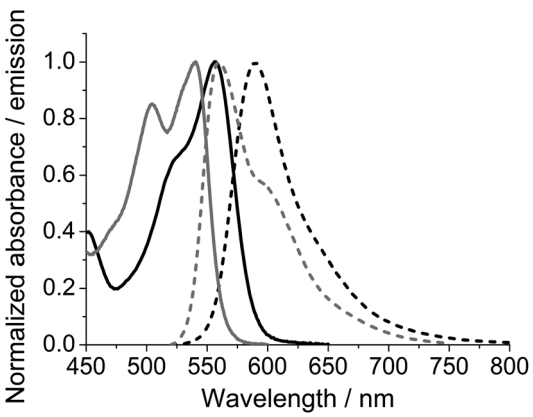

Fig. 1 Absorption (full) and emission (dashed) spectra of ADOTA **4c** (grey) and DAOTA **5c** (black) measured in acetonitrile solution.

Table 1 Photophysical properties of *N*-(4-carboxyphenyl)-azadioxatriangulenium tetrafluoroborate (ADOTA, **4c**) and *N*-(4-carboxyphenyl)-*N*′-methyl-diazaoxatriangulenium tetrafluoroborate (DAOTA, **5c**) in acetonitrile (MeCN), dimethyl sulfoxide (DMSO), and phosphate buffered saline at pH = 7.4 (PBS) solutions

	ADOTA **4c**			DAOTA **5c**		
Solvent	MeCN	DMSO	PBS	MeCN	DMSO	PBS
λ_{abs}/nm	536	539	539	557	561	556
λ_{em}/nm	562	570	560	590	600	592
$\Delta_{Stokes'}$/nm	26	31	21	33	39	36
τ_{fl}/ns	21.0	17.1	17.9	18.7	15.1	14.0
ϕ_{fl}	0.64	0.64	0.57	0.55	0.45	0.35
τ^0/ns	32.8	26.7	31.4	34.0	33.6	40.0

λ_{abs} is the wavelength of the lowest energy absorption maximum given in nm. λ_{em} is the wavelength at the emission maximum given in nm, $\Delta_{Stokes'}$ is the Stokes' shift given in nm, τ_{fl} is the fluorescence lifetime given in ns, and ϕ_{fl} is the measured fluorescence quantum yield using rhodamine 6G as a reference, τ^0 is the radiative lifetime: τ_{fl}/ϕ_{fl} given in ns.

The fluorescence lifetime (τ_{fl}) for DAOTA **5c** is exceptionally long for a red emitting organic dye, even when reduced to 14 ns by unspecific solvent quenching in PBS solution. The combination of a long fluorescence lifetime (>10 ns) and emission in the red (>600 nm) makes DAOTA ideally suited to monitor rotational correlation times of biomolecules and as a fluorescent probe for fluorescence polarisation based assays.[8,47–49]

DAOTA-BSA conjugates

To test the ability of DAOTA as a probe for measuring the rotational motion of proteins the reactive ester of DAOTA **5c**, *N*-(4-carboxyphenyl)-*N*′-methyl-diazaoxatriangulenium NHS ester tetrafluoroborate **6c**, was conjugated to BSA. This reaction is expected to predominately result in conjugation of the triangulenium based probe to the *N*-terminus of the protein.[46] The labelling protocol was optimised to give a low degree of labelling (DOL) to ensure that complications arising from multiple labels, such as energy transfer between labels, was minimal. When developing a fluorescence polarisation assay, these effects can be probed by looking for Weber's red-edge effect.[67,68] A DOL of 0.9 DAOTA dyes per BSA was used to obtain the results presented below.

The Perrin equation (eqn (2)) describes the ideal relationship between: the observed fluorescence anisotropy (r), the fundamental anisotropy of the dye (r_0), the rotational correlation time of the rotating volume (θ), and the fluorescence lifetime (τ_{fl}). The rotational correlation time (θ) is directly related (eqn (3)) to the rotational volume (V) and the viscosity of the surrounding

medium (η). For proteins, the rotational correlation time can be related (eqn (3)) to the molecular mass (M), the specific density (ν), and the average hydration (h) of the protein.[66]

$$r_0/r = 1 + \tau_{fl}/\theta \quad (2)$$

$$\theta = \eta V/RT = \eta M/RT \cdot (\nu + h) \quad (3)$$

Two factors related to the fluorescent probe used are found in the equations: the fluorescence lifetime (τ_{fl}) and the fundamental fluorescence anisotropy (r_0). The fluorescence lifetime determines the range of rotational correlation times that may be probed, in other words the range of molecular weights that can be investigated. The fundamental anisotropy, ranging from 0.4 to −0.2, determines the dynamic range of the experiments. Dyes with a low r_0 value are poor probes for fluorescence polarisation-based methods. DAOTA has r_0 = 0.38,[65] which is very close to the maximal value (0.4), while the fluorescence lifetime allows for probing biomolecules with a molecular weight up towards 1000 kDa.[46]

Fig. 2 shows a Perrin plot of **5c** conjugated to BSA (**5c**-BSA), where the steady-state fluorescence anisotropy (r) measured at four different temperatures (T) are plotted as $1/r$ against T/η and used to determine the θ/V, and the apparent anisotropy (r_0^{app}) by extrapolation of T/η to zero. The latter is a measure for the flexibility of the dye label, when conjugated to the biomolecule. Ideally, if the label upon conjugation loses all degrees of freedoms, except co-rotation with the biomolecule, the apparent and fundamental anisotropy will be identical. Any local flexibility of the dye label will induce a pathway for fast scrambling of the photoselection not related to the motion of the biomolecule. The result is a lowering of the apparent anisotropy r_0^{app} in a Perrin plot, and a loss of dynamic range in any fluorescence polarisation based experiment. For **5c**-BSA the apparent anisotropy is at r_0^{app} = 0.36 surprisingly high, clearly indicating that the DAOTA label is immobilised on the surface of BSA.

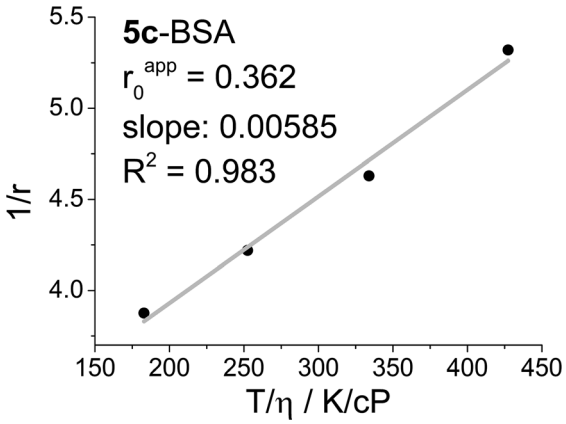

Fig. 2 Perrin plot of **5c**-BSA in phosphate buffered saline at pH = 7.4 solution. The experiment was performed on a sample with a DOL = 0.9, where the steady state fluorescence anisotropy (r) was determined at four different temperatures (T).

While the effect of the long fluorescence lifetime of **5c** may be hard to identify in the steady state spectra, it is directly visible in time-resolved experiments. Fig. 3 (top) shows a time-resolved emission decay profile for **5c** and **5c**-BSA measured in PBS solution, obtained using time-correlated single photon counting (TCSPC). Cursory inspection of the fluorescence decays profiles in Fig. 3 (top) shows that the **5c**-BSA has a longer fluorescence lifetime than **5c** in PBS solution ($\tau_{fl,5c}$ = 14.0 ns *vs.* $\tau_{fl,5c\text{-}BSA}$ 21.2 ns, see ESI†), and that photons can be detected well beyond 150 ns when using the standard settings of TCSPC with a maximum count of 10.000. By using longer acquisition times (higher maximum number of counts), photons arising from emission of the **5c**-BSA conjugates may be detected up towards 250 ns after excitation, this is without equal when considering organic dyes with emission in the red.

Fig. 3 (bottom) shows the time-resolved anisotropy decay for **5c**-BSA. The data allow for direct determination of the rotational correlation time of the rotating volume (θ). The long fluorescence lifetime is important in obtaining these data, as photons must be emitted in a time interval long enough to describe the rotational motion of the biomolecule. Fig. 3b

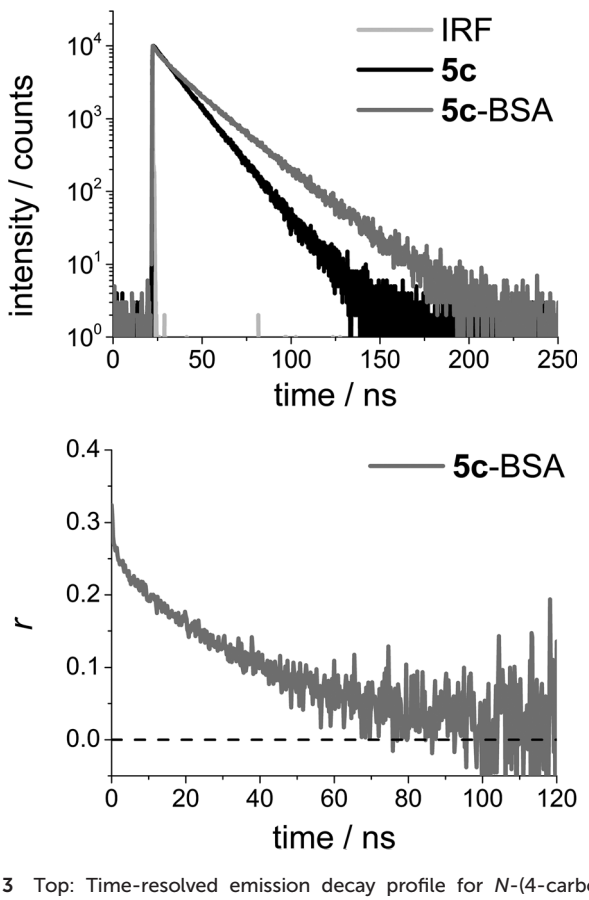

Fig. 3 Top: Time-resolved emission decay profile for *N*-(4-carboxyphenyl)-*N*′-methyl-diazaoxatriangulenium tetrafluoroborate (DAOTA, **5c**) and the corresponding BSA conjugate (**5c**-BSA) measured in PBS solution. Bottom: Time-resolved anisotropy decay profile for **5c**-BSA measured in PBS solution. For details on fits and the resulting parameters see the ESI.†

shows that in the case of **5c**-BSA the photoselection is fully scrambled by rotational motion in ~100 ns. That is, the anisotropy has decayed to zero. The long rotational correlation time determined for BSA from these data is θ_{BSA} = 40 ns (see ESI for details†), a number identical to the average literature value of θ_{BSA} = 40 ns.[69] Note that BSA is not a perfect spherical rotor, and the value determined will be influenced by the position and relative orientation of the dye in the bioconjugate.

While emission from either of the azaoxa-triangulenium dyes can be used to follow the rotational motion of large biomolecules for more than 100 ns,[27] there is a clear difference in the behaviour of **4a**-BSA and **5c**-BSA. Where ADOTA fluorescence is quenched in the conjugates (**4a**-BSA) when compared to the non-bounded dyes (**4a**), the DAOTA fluorescence appears to be enhanced upon conjugation, as seen by the significantly increased fluorescence lifetime (Fig. 3). As the fluorescence lifetime only report on the emitting population of dyes, the actual emission intensity of each dye was determined. Fig. 4 shows the results for **4a**-BSA and **5c**-BSA. The total emission intensity of either dye is decreased upon conjugation to BSA, but the effect is much less pronounced for the DAOTA derivative. We rationalised the quenching of the ADOTA fluorescence as a result of reductive PET quenching by tryptophan,[50] a process the increased cation stability of DAOTA makes less favoured (see ESI for details†).[53] Thus, we see less quenching of the DAOTA fluorescence in the **5c**-BSA conjugates. The significant increase in lifetime upon conjugation of **5c** to BSA must be due to a reduction in the non-specific solvent induced quenching of a population of DAOTA dyes that is partially shielded by the protein surface, while the reduction in overall intensity must be due to an almost fully quenched population of **5c**-BSA. The quenched population does not contribute to the time-resolved emission decay profile, and will not influence the fluorescence anisotropy. The net result is that the fluorescence quantum yield of the **5c**-BSA conjugate at ϕ_{fl} = 0.34 is very close to that of the free dye **5c** in PBS at ϕ_{fl} = 0.35, although with a more complicated time-resolved fluorescence decay profile (see ESI†).

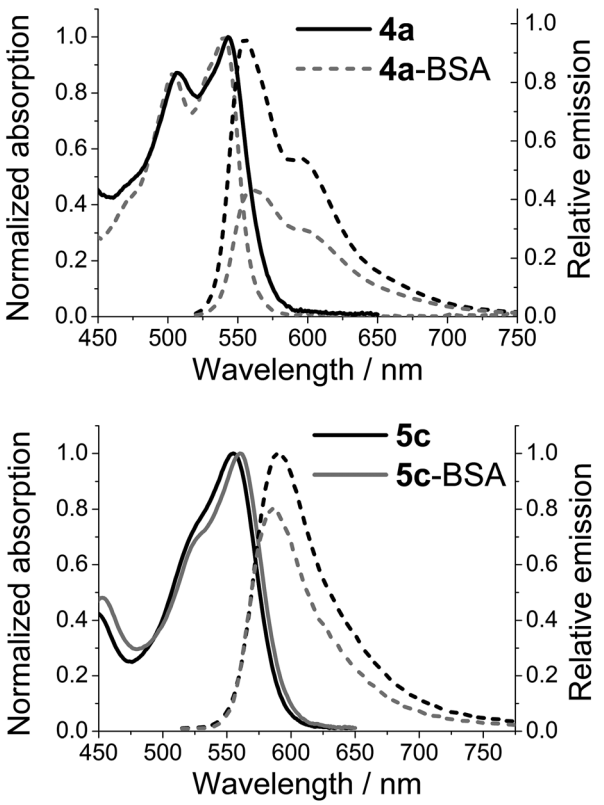

Fig. 4 Normalised absorption spectra (full) and relative emission spectra (dashed) of **4a** and **4a**-BSA (top) and **5c** and **5c**-BSA (bottom) measured in PBS solution. The absorption spectra are normalised at λ_{max}, while the emission is normalised by the absorption at the point of excitation.

Conclusions

The syntheses of six new derivatives of diazaoxatriangulenium (DAOTA) salts were reported, and it was shown that these dyes can be accessed *via* two synthetic routes. One set of substituents may favour one route over the other.

The photophysical properties of the DAOTA fluorophore were investigated in view of using the red emitting, long fluorescence lifetime dye in fluorescence polarisation assays. We showed that the DAOTA fluorophore undergoes unspecific solvent fluorescence quenching in aqueous buffer, reducing the fluorescence lifetime from 19 ns in acetonitrile solution to 14 ns in PBS solution. **5c** was conjugated to BSA, and we found that **5c**-BSA had a significantly increased longest fluorescence lifetime component at 21.2 ns (as well as intensity weighted average fluorescence lifetime of 19.2 ns). Furthermore, the overall emission intensity of the conjugates (**5c**-BSA) was found to be equal to that of the free dye (**5c**) measured in PBS solution, as **5c** is less quenched by tryptophan. Thus the DAOTA fluorophore, with emission further in the red and a longer fluorescence lifetime in biomolecule conjugates, was found to be superior to the ADOTA fluorophore as a probe for developing fluorescence polarisation assays for large biomolecules.

Acknowledgements

The authors thank the University of Copenhagen, the National Institute of Health (USA) NIH Grant: R01EB12003, the Carlsberg Foundation, the Villum Foundation, DFF|FTP, and the Danish National Research Foundation under the Danish-Chinese Centre for Self-Assembled Molecular Electronic Nanosystems for financial support. M.R. is grateful to the Danish Council of Independent Research for financial support.

Notes and references

1 B. R. Hurley and C. D. Regillo, *Fluorescein Angiography: General Principles and Interpretation*, Springer, New York, 2009.

2 D. M. Jameson and J. A. Ross, *Chem. Rev.*, 2010, **110**, 2685–2708.
3 S. M. Borisov and O. S. Wolfbeis, *Chem. Rev.*, 2008, **108**, 423–461.
4 O. S. Wolfbeis, *Anal. Chem.*, 2008, **80**, 4269–4283.
5 L. M. Smith, J. Z. Sanders, R. J. Kaiser, P. Hughes, C. Dodd, C. R. Connell, C. Heiner, S. B. H. Kent and L. E. Hood, *Nature*, 1986, **321**, 674–679.
6 J. Inglese, R. L. Johnson, A. Simeonov, M. Xia, W. Zheng, C. P. Austin and D. S. Auld, *Nat. Chem. Biol.*, 2007, **3**, 466–479.
7 S. Weiss, *Nat. Struct. Biol.*, 2000, **7**, 724–729.
8 J. C. Owicki, *J. Biomol. Screening*, 2000, **5**, 297–306.
9 S. Viswanathan, M. E. Williams, E. B. Bloss, T. J. Stasevich, C. M. Speer, A. Nern, B. D. Pfeiffer, B. M. Hooks, W. P. Li, B. P. English, T. Tian, G. L. Henry, J. J. Macklin, R. Patel, C. R. Gerfen, X. Zhuang, Y. Wang, G. M. Rubin and L. L. Looger, *Nat. Methods*, 2015, **12**, 568–576.
10 K. D. Wegner and N. Hildebrandt, *Chem. Soc. Rev.*, 2015, **44**, 4792–4834.
11 E. G. Moore, A. P. Samuel and K. N. Raymond, *Acc. Chem. Res.*, 2009, **42**, 542–552.
12 T. Yoshihara, Y. Yamaguchi, M. Hosaka, T. Takeuchi and S. Tobita, *Angew. Chem., Int. Ed.*, 2012, **51**, 4148–4151.
13 J. B. Grimm, B. P. English, J. Chen, J. P. Slaughter, Z. Zhang, A. Revyakin, R. Patel, J. J. Macklin, D. Normanno, R. H. Singer, T. Lionnet and L. D. Lavis, *Nat. Methods*, 2015, **12**, 244–250.
14 B. N. G. Giepmans, S. R. Adams, M. H. Ellisman and R. Y. Tsien, *Science*, 2006, **312**, 217–224.
15 I. Johnson, *Histochem. J.*, 1998, **30**, 123–140.
16 A. P. de Silva, H. Q. N. Gunaratne, T. Gunnlaugsson, A. J. M. Huxley, C. P. McCoy, J. T. Rademacher and T. E. Rice, *Chem. Rev.*, 1997, **97**, 1515–1566.
17 R. Meyer, *Z. Phys. Chem.*, 1897, **24**, 468–508.
18 L. M. Wysocki and L. D. Lavis, *Curr. Opin. Chem. Biol.*, 2011, **15**, 752–759.
19 S. W. Yun, N. Y. Kang, S. J. Park, H. H. Ha, Y. K. Kim, J. S. Lee and Y. T. Chang, *Acc. Chem. Res.*, 2014, **47**, 1277–1286.
20 H. Kobayashi, M. Ogawa, R. Alford, P. L. Choyke and Y. Urano, *Chem. Rev.*, 2009, **110**, 2620–2640.
21 A. Loudet and K. Burgess, *Chem. Rev.*, 2007, **107**, 4891–4932.
22 *Advanced Fluorescence Reporters in Chemistry and Biology II*, ed. A. P. Demchenko, Series ed. O. S. Wolfbeis, Springer, Berlin, Heidelberg, 2010.
23 *Advanced Fluorescence Reporters in Chemistry and Biology I*, ed. A. P. Demchenko, Series ed. O. S. Wolfbeis, Springer, Berlin, Heidelberg, 2010.
24 T. Myochin, K. Hanaoka, S. Iwaki, T. Ueno, T. Komatsu, T. Terai, T. Nagano and Y. Urano, *J. Am. Chem. Soc.*, 2015, **137**, 4759–4765.
25 E. Kim, Y. Lee, S. Lee and S. B. Park, *Acc. Chem. Res.*, 2015, **48**, 538–547.
26 E. Heyer, P. Lory, J. Leprince, M. Moreau, A. Romieu, M. Guardigli, A. Roda and R. Ziessel, *Angew. Chem., Int. Ed.*, 2015, **54**, 2995–2999.
27 M. Tasior, Y. M. Poronik, O. Vakuliuk, B. Sadowski, M. Karczewski and D. T. Gryko, *J. Org. Chem.*, 2014, **79**, 8723–8732.
28 P. Shieh, M. S. Siegrist, A. J. Cullen and C. R. Bertozzi, *Proc. Natl. Acad. Sci. U. S. A.*, 2014, **111**, 5456–5461.
29 A. Poirel, P. Retailleau, A. De Nicola and R. Ziessel, *Chem. – Eur. J.*, 2014, **20**, 1252–1257.
30 G. Lukinavicius, L. Reymond, E. D'Este, A. Masharina, F. Gottfert, H. Ta, A. Guther, M. Fournier, S. Rizzo, H. Waldmann, C. Blaukopf, C. Sommer, D. W. Gerlich, H. D. Arndt, S. W. Hell and K. Johnsson, *Nat. Methods*, 2014, **11**, 731–733.
31 Y.-L. Huang, A. S. Walker and E. W. Miller, *J. Am. Chem. Soc.*, 2015, **137**, 10767–10776.
32 J. Bosson, J. Gouin and J. Lacour, *Chem. Soc. Rev.*, 2014, **43**, 2824–2840.
33 B. W. Laursen, F. C. Krebs, M. F. Nielsen, K. Bechgaard, J. B. Christensen and N. Harrit, *J. Am. Chem. Soc.*, 1998, **120**, 12255–12263.
34 B. W. Laursen and T. J. Sørensen, *J. Org. Chem.*, 2009, **74**, 3183–3185.
35 T. J. Sørensen and B. W. Laursen, *J. Org. Chem.*, 2010, **75**, 6182–6190.
36 F. Westerlund, C. B. Hildebrandt, T. J. Sørensen and B. W. Laursen, *Chem. – Eur. J.*, 2010, **16**, 2992–2996.
37 B. W. Laursen and F. C. Krebs, *Angew. Chem., Int. Ed.*, 2000, **39**, 3432–3434.
38 B. W. Laursen and F. C. Krebs, *Chem. – Eur. J.*, 2001, **7**, 1773–1783.
39 T. J. Sørensen, B. W. Laursen, R. Luchowski, T. Shtoyko, I. Akopova, Z. Gryczynski and I. Gryczynski, *Chem. Phys. Lett.*, 2009, **476**, 46–50.
40 P. Hammershøj, T. J. Sørensen, B.-H. Han and B. W. Laursen, *J. Org. Chem.*, 2012, **77**, 5606–5612.
41 A. Shivalingam, M. A. Izquierdo, A. L. Marois, A. Vysniauskas, K. Suhling, M. K. Kuimova and R. Vilar, *Nat. Commun.*, 2015, **6**, 8178.
42 M. B. Smith and J. March, in *March's Advanced Organic Chemistry*, Wiley, New York, 5th edn, 2001, ch. 13, pp. 850–893.
43 M. Bhanuchandra, K. Murakami, D. Vasu, H. Yorimitsu and A. Osuka, *Angew. Chem., Int. Ed.*, 2015, **54**, 10234–10238.
44 J. C. Martin and R. G. Smith, *J. Am. Chem. Soc.*, 1964, **86**, 2252–2256.
45 M. E. Smith, M. B. Caspersen, E. Robinson, M. Morais, A. Maruani, J. P. Nunes, K. Nicholls, M. J. Saxton, S. Caddick, J. R. Baker and V. Chudasama, *Org. Biomol. Chem.*, 2015, **13**, 7946–7949.
46 S. A. Bogh, I. Bora, M. Rosenberg, E. Thyrhaug, B. W. Laursen and T. J. Sørensen, *Methods Appl. Fluoresc.*, 2015, **3**, 045001.
47 I. Bora, S. A. Bogh, M. Santella, M. Rosenberg, T. J. Sørensen and B. W. Laursen, *Eur. J. Org. Chem.*, 2015, 6351–6358, DOI: 10.1002/ejoc.201500888.
48 T. J. Sørensen, E. Thyrhaug, M. Szabelski, R. Luchowski, I. Gryczynski, Z. Gryczynski and B. W. Laursen, *Methods Appl. Fluoresc.*, 2013, **1**, 025001.

49 B. P. Maliwal, R. Fudala, S. Raut, R. Kokate, T. J. Sørensen, B. W. Laursen, Z. Gryczynski and I. Gryczynski, *PLoS One*, 2013, **8**, e63043.
50 S. Doose, H. Neuweiler and M. Sauer, *ChemPhysChem*, 2005, **6**, 2277–2285.
51 A. C. Vaiana, H. Neuweiler, A. Schulz, J. Wolfrum, M. Sauer and J. C. Smith, *J. Am. Chem. Soc.*, 2003, **125**, 14564–14572.
52 N. Marme, J. P. Knemeyer, M. Sauer and J. Wolfrum, *Bioconjugate Chem.*, 2003, **14**, 1133–1139.
53 S. Dileesh and K. R. Gopidas, *J. Photochem. Photobiol., A*, 2004, **162**, 115–120.
54 M. Sauer, K. T. Han, R. Müller, S. Nord, A. Schulz, S. Seeger, J. Wolfrum, J. Arden-Jacob, G. Deltau, N. J. Marx, C. Zander and K. H. Drexhage, *J. Fluoresc.*, 1995, **5**, 247–261.
55 M. Sauer, K. T. Han, R. Müller, A. Schulz, R. Tadday, S. Seeger, J. Wolfrum, J. Arden-Jacob, G. Deltau, N. J. Marx and K. H. Drexhage, *J. Fluoresc.*, 1993, **3**, 131–139.
56 R. P. Haugland, *Handbook of Fluorescent Probes and Research Chemicals*, Molecular Probes, Eugene, Oregon, 11th edn, 2010.
57 N. Panchuk-Voloshina, R. P. Haugland, J. Bishop-Stewart, M. K. Bhalgat, P. J. Millard, F. Mao and W. Y. Leung, *J. Histochem. Cytochem.*, 1999, **47**, 1179–1188.
58 C. Würth, M. Grabolle, J. Pauli, M. Spieles and U. Resch-Genger, *Nat. Protocols*, 2013, **8**, 1535–1550.
59 A. M. Brouwer, *Pure Appl. Chem.*, 2011, **83**, 2213–2228.
60 C. Nicolas, G. Bernardinelli and J. Lacour, *J. Phys. Org. Chem.*, 2010, **23**, 1049–1056.
61 G. D. Figuly, C. K. Loop and J. C. Martin, *J. Am. Chem. Soc.*, 1989, **111**, 654–658.
62 F. C. Krebs, H. Spanggaard, N. Rozlosnik, N. B. Larsen and M. Jørgensen, *Langmuir*, 2003, **19**, 7873–7880.
63 T. J. Sørensen, C. B. Hildebrandt, M. Glyvradal and B. W. Laursen, *Dyes Pigm.*, 2013, **98**, 297–303.
64 G. T. Hermanson, *Bioconjugate Techniques*, Academic Press, Oxford, 2013.
65 E. Thyrhaug, T. J. Sørensen, I. Gryczynski, Z. Gryczynski and B. W. Laursen, *J. Phys. Chem. A*, 2013, **117**, 2160–2168.
66 J. R. Lakowicz, *Principles of Fluorescence Spectroscopy*, Springer-Verlag, New York Inc., New York, 3. Revised edn, 2006.
67 G. Weber and M. Shinitzky, *Proc. Natl. Acad. Sci. U. S. A.*, 1970, **65**, 823–830.
68 B. D. Hamman, A. V. Oleinikov, G. G. Jokhadze, R. R. Traut and D. M. Jameson, *Biochemistry*, 1996, **35**, 16680–16686.
69 M. L. Ferrer, R. Duchowicz, B. Carrasco, J. G. D. L. Torre and A. U. Acuna, *Biophys. J.*, 2001, 2422–2430.